Rate of Carotenoid Triplet Formation in Solubilized Light-Harvesting Complex II (LHCII) from Spinach

René Schödel,* Klaus-D. Irrgang,# Joachim Voigt,* and Gernot Renger#
*AG Molekulare Biophysik und Spektroskopie, Institut für Physik der Humboldt Universität zu Berlin, and #Max-Volmer-Institut für Biophysikalische Chemie und Biochemie, Technische Universität Berlin, Berlin, Germany

ABSTRACT In the present study the rate of triplet transfer from chlorophyll to carotenoids in solubilized LHCII was investigated by flash spectroscopy using laser pulses of ~2 ns for both pump and probe. Special attention has been paid to calibration of the experimental setup and to avoid saturation effects. Carotenoid triplets were identified by the pronounced positive peak at ~507 nm in the triplet-singlet difference spectra. ΔOD (507 nm) exhibits a monoexponential relaxation kinetics with characteristic lifetimes of 2–9 μs (depending on the oxygen content) that was found to be independent of the pump pulse intensity. The rise of ΔOD (507 nm) was resolved via a pump probe technique where an optical delay of up to 20 ns was used. A thorough analysis of these experimental data leads to the conclusion that the kinetics of carotenoid triplet formation in solubilized LHCII is almost entirely limited by the lifetime of the excited singlet state of chlorophyll but neither by the pulse width nor by the rate constant of triplet-triplet transfer. Within the experimental error the rate constant of triplet-triplet transfer from chlorophyll to carotenoids was estimated to be $k_{TT} > (0.5\ \text{ns})^{-1}$. This value exceeds all data reported so far by at least one order of magnitude. The implications of this finding are briefly discussed.

INTRODUCTION

The capability of adaptation to different illumination conditions is most important for both high efficiency of solar radiation exploitation and survival of cyanobacteria and plants under light stress. Both demands are satisfied by operational units referred to as antenna systems. Different types of antenna systems have been developed. They consist of pigment-protein complexes that are either incorporated into the membrane as integral proteins or bound as extrinsic units (for reviews see Gantt, 1986; Thornber et al., 1991). The most abundant light-harvesting complex (LHC) is LHCIIb, which binds ~50% of the total chlorophyll (Chl) content of the thylakoid membrane. This complex is normally isolated in trimers that are assumed to be also the predominant form of LHCIIb in vivo. Together with minor pigment-protein complexes (each containing ≤5% Chl), LHCIIb constitutes an oligomeric system that is incorporated into the membrane and builds up the peripheral and proximal antenna of photosystem II (PS II) in green plants (Kühlbrandt, 1994; Jansson, 1994; Zuchelli et al., 1994; Paulsen, 1995; Green et al., 1996).

Regardless of the detailed structure, antenna systems generally capture the few photons available at low light intensities with a large overall optical cross section. The electronically excited states formed by light absorption are rapidly funneled almost without loss to the photochemically active pigment of the reaction center. This process occurs via a sequence of very fast transfer steps that comprise almost entirely the levels of the first excited singlet states of the pigments (for reviews see Renger, 1992; van Grondelle et al., 1994). A complex regulatory mechanism permits via lateral diffusion of phosphorylated LHCII an optimal distribution of excitation energy between PS I and PS II (see Allen and Nilsson, 1997, and references therein). An oppositive function to light harvesting is required at high light intensities. In this case the superfluous energy has to be dissipated to heat to minimize deleterious effects, owing to photoinhibition. This goal is achieved by formation of channels in the antenna for radiationless decay of excited states (for recent review see Horton et al., 1996).

Among the pigments participating in the antenna reactions, carotenoids are of paramount importance (for a recent review see Frank and Cogdell, 1996). These molecules exert multiple functions: 1) they act as accessory pigments in the very fast singlet-singlet energy transfer (Connelly et al., 1997) to antenna chlorophylls and eventually the reaction center, thereby extending the spectral range of absorption, 2) carotenoids are essential for the assembly of LHCII (Heinze et al., 1997), 3) in the violaxanthin-zeaxanthin cycle carotenoids play a key role in the mechanism of nonphotochemical quenching (Demming-Adams et al., 1995; Horton et al., 1996), and 4) the most important and indispensable function is the protection against damage by singlet oxygen (for a review see Siefermann-Harms, 1987). Carotenoids are especially suited because they provide a twofold protection. First, carotenoids can act as efficient quenchers of chlorophyll triplets that cause the sensitized formation of singlet oxygen ($^1\Delta_g O_2$). Second, carotenoids rapidly degrade $^1\Delta_g O_2$ into the ground state $^3\Sigma_g O_2$ (Foote, 1976). The carotenoid triplets formed in both quenching reactions decay radiationless into the ground state.

Received for publication 2 February 1998 and in final form 8 September 1998.

Address reprint requests to Dr. René Schödel, Institut für Physik der Humboldt Universität zu Berlin, Invalidenstrasse 110, 10115 Berlin, Germany. Tel.: 49-30-2093-7668; Fax: 49-30-2093-7659; E-mail: schoedel@physik.hu-berlin.de.

0006-3495/98/12/3143/11 $2.00

The triplet-triplet energy transfer from ^{3}Chl to ^{1}Car requires a Dexter-type exchange mechanism and is therefore restricted to rather short distances between both molecules (see Renger, 1992; van Grondelle, 1994).

The structure of LHCII has been recently resolved to 3.4 Å by electron diffraction of two-dimensional crystals (Kühlbrandt et al., 1994). It shows that the closest distance between the two xanthophylls (assigned to luteins) forming an internal cross-brace and the nearest chlorophyll is ~4 Å. Therefore, the conditions for an efficient Dexter-type mechanism are satisfied. Indeed, the efficiency of Chl triplet quenching by xanthophylls in LHCII was recently shown to be close to 100% at room temperature (Peterman et al., 1995). Based on previous measurements the rate constant for this process was estimated to be $(10\ \text{ns})^{-1}$ (Kramer and Mathis, 1980). This value is of the same order of magnitude as the rate of ^{3}Chl formation by intersystem crossing. It is therefore interesting to analyze to what extent the latter process affects the overall reaction. To address this point, pump-probe experiments were performed with solubilized LHCII. As a surprising result of the data analyses, the molecular rate constant for the excitation energy transfer from ^{3}Chl to ^{1}Car was found to be at least $(0.5\ \text{ns})^{-1}$. This value exceeds the data reported so far by more than one order of magnitude.

MATERIALS AND METHODS

Sample material

PS II membrane fragments were isolated from spinach according to the method of Berthold et al. (1981) with some modifications as outlined in Völker et al., 1985. The isolation of LHCII was performed in the presence of β-dodecylmaltoside as described in detail (Irrgang et al., 1988). The LHCII preparations were characterized by room temperature absorption spectroscopy using a Shimadzu UV 3000 spectrophotometer. Absorption maxima in the red were localized at 652 ± 1 and 675 ± 1 nm. Pigment concentration and Chl *a*/*b* ratio were determined by using the method of Porra et al., 1989. The latter value was found to be 1.35 ± 0.05. The polypeptide composition of the LHCII preparation has been checked by SDS/urea-PAGE using the method described in Irrgang et al., 1988. The relative amount of the apoproteins of the various Chl protein complexes identified in the LHCII preparations used in the study have been estimated from scanning of silver-stained SDS/urea/polyacrylamide gels using a Desaga Quick scan densitometer; 87.4% of the apoproteins could be ascribed to the lhcb1–3 gene products and 12.6% to the minor pigment protein complexes lhcb5/lhcb6. Only traces of the lhcb4 protein were detected.

The LHCII preparation was diluted with a buffer containing: 30 mM MES-NaOH, pH 6.5, 10 mM $CaCl_2$, 20% w/v sucrose, and 0.025% w/v β-dodecylmaltoside. The total chlorophyll concentration of the sample was 0.20 mg of Chl/cm^3.

The content of β-carotene and xanthophylls has been spectrophotometrically determined by measuring the absorbance at 470 nm in 80% v/v acetone. The calculations were carried out using the equation described in Wellburn and Lichtenthaler (1984). The carotenoid composition of the samples was analyzed by RP-HPLC using a Nucleosil 100 C-18 column (Knauer, Berlin, Germany; (25 cm × 4.0 mm; inner diameter, 5 μm) in combination with methanol/tetrahydrofuran (9/1 (v/v)) as solvent. The pigments were separated at a flow rate of 1 ml/min. Elution was followed at 450 nm. Chl *a* (Fluka, Deisenhofen, Germany), lutein (Sigma, Deisenhofen, Germany), and β-carotene (Fluka) were applied as external and internal standards. The average pigment composition of the LHCII samples (n = 10) used was investigated using HPLC analysis resulting in the following: 0.2 lutein, 0.078 violaxanthin, 0.078 neoxanthin, 0.015 β-carotene per Chl *a* (mol/mol). These values are similar to those described by Peterman et al. (1997b) and Bassi et al. (1993) for LHCII of maize. The highest variability in the content of carotenoids was found for neoxanthin. Some samples did not even contain any neoxanthin. They have not been used for this study. The lability of the binding of neoxanthin has also been established by Kühlbrandt et al. (1994). Possibly neoxanthin is located in the periphery of the pigment protein complex.

The LHCII preparation contains solubilized nonaggregated complexes. Two different lines of experimental evidence strongly support the presence of trimeric complexes and the absence of aggregates. 1) The fluorescence emission spectra at 77 K show a narrow band at 681 nm with a free width at half-magnitude of 9 nm, which is characteristic for the trimeric form (see also Vasil'ev et al., 1997a; Peterman et al., 1996; Hemelrijk et al., 1992), and 2) no additional fluorescence emission bands could be observed at wavelengths of 712 or 738 nm, indicating that no aggregated pigment complexes were present. Aggregates can easily be obtained after dialysis of the complexes removing the detergent used for isolating the complex (β-dodecylmaltoside) (see Vasil'ev et al., 1997a).

In LHCII, aerobic/anaerobic conditions were obtained by exposure of the sample to wet air/nitrogen gas at room temperature.

Commercially available Chl *b* from spinach (Sigma) was dissolved in a mixture of 80% v/v acetone (Roth GmbH and Co., Karloruhe, Germany; HPLC grade). The concentration was ~0.2 mg Chl/cm^3 (~0.22 mM).

Experimental setup

A schematic description of home-built equipment used for one-color experiments is shown in Fig. 1. Pulses with spectral width of 0.3 nm and a maximal energy of ~20 μJ were generated by a compact N_2/dye laser

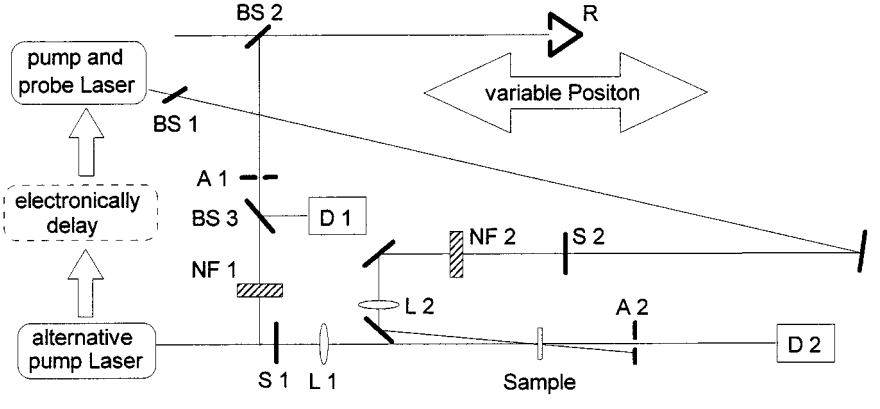

FIGURE 1 Scheme of the optical arrangement of home-built equipment. For a description see text. BS, beam splitter; A, aperture; R, retroreflector; D, detector; L, lens; NF, wheels with neutral density filters; S, automatic shutter.

module (VSL-dye, Laser Science, Newton, MA) at a repetition rate of up to 20 Hz. The beam divergence was <0.5 mrad. The pulse train was divided into a pump and probe beam. The pump beam reached the sample with an angle of ~1° with respect to the probe beam. This arrangement permitted a complete spatial separation of the signal at detector D2 from the pump beam. The time between pump and probe pulses was adjusted by a variable optical delay line via a retro reflector (Spindler and Hoyer, Göttingen, Germany). The maximal delay used in these experiments was 20 ns. Accordingly, the difference in optical path length had to be varied up to 6 m. The size of both spots was determined as described in Schödel et al. (1996). The diameter of the spot produced by the pump beam was ~300 μm to ensure that it was large enough to avoid a displacement of the spot monitored by the probe pulse through the sample. The intensity of the probe pulse chosen was approximately three orders of magnitude below that of the pump pulse. To cope with variations in pulse intensity, the probe beam was split to obtain a reference signal at detector 1, thereby permitting a suitable normalization of the data.

The relative change of the optical density ΔOD was determined for each delay time between pump and probe pulse in the following way. The signals of the detectors D1 and D2 were transferred into a boxcar integrator and the integrated values stored on a PC. For each probe pulse a home-made measuring program was used to determine the ratio of the signals from detector 2 by reference detector 1 before averaging. This procedure was performed with and without pump pulse to determine the value of the relative change of the transmittance T^{rel}. The value of ΔOD was determined from the decadic logarithm: $\Delta OD = -\lg(T^{rel})$.

The time course of excitation was measured with a fast microchannel multiplier and a high-frequency oscilloscope (Tektronix 684A), which allowed us to observe single pulses. It was found that the pulses can approximately be described by a Gaussian profile with $\Delta \sim 1.1$ ns. Then the time dependence of the pump and probe pulse is given by:

$$i^{pump/probe}(t) = \Gamma(t) I^{pump/probe} \quad (1)$$

with

$$\Gamma(t) = \frac{1}{\Delta \cdot \sqrt{2 \cdot \pi}} e^{-t^2/2 \cdot \Delta^2} \quad (2)$$

I^{pump} and I^{probe} are integrated photon densities of the pulses (in units of photons cm^{-2} $pulse^{-1}$). The intensity of the pump pulse was adjusted to the desired value by using neutral density filters as described by Schödel et al. (1996).

For the measurements of the triplet minus singlet (T − S) difference spectra and μs kinetics, the same beam geometry with respect to the sample was used. The pump pulses at a wavelength of 645 nm were provided by a Nd^{3+}-YAG-laser pumped dye laser (LAS LDL 105), which triggered the N_2/dye laser as the source of the probe pulses. To cope with the whole wavelength region (400–710 nm), six different laser dyes (Stilben 3, Courmarin 2, Courmari 307, Rhodamin 6G, DCM, and Pyridin) were used. The difference spectra were recorded at a fixed delay of 50 ns between pump and probe pulse. For monitoring the slow (μs) decay kinetics at a fixed wavelength of the probe pulse, the delay between pump and probe pulse was varied via a programmable home-built electronic unit. The time resolution of this type of experiment was limited by the jitter of ~±10 ns between pump and probe pulse. The kinetics of ΔOD at various probe wavelengths was measured in a 1-mm cuvette.

RESULTS AND DISCUSSION

Triplet minus singlet difference spectrum

Fig. 2 shows the spectrum of flash-induced absorption changes measured at 50 ns after the actinic flash in solubilized LHCII. The fluorescence lifetime of this sample type was found to be 4.3 ns (Vasil'ev et al., 1997b). Therefore, at 50 ns the difference spectrum does not contain any contributions from excited singlet states and represents the T − S difference spectrum. The shape of the spectrum with a pronounced peak at 507 nm is virtually the same as that reported by Nechushtai et al. (1988) and recently by Peterman et al. (1995) for LHCII solubilized by a different procedure. This finding indicates that the room temperature T − S spectrum is not very sensitive to the method of LHCII preparation. Except for a small bleaching in the Q_y region of Chl *a* (around 675 nm), the features of the spectrum are typical for the T − S spectrum of carotenoids.

Relaxation of carotenoid triplets

To check for the lifetime of ^{3}Car, the relaxation kinetics were measured at 507 and 530 nm. The rise kinetics cannot be resolved at the time resolution (tens of nanoseconds) of the equipment used for these experiments (see Materials and Methods). Fig. 3 shows traces measured at 507 and 530 nm in anaerobic and fully aerobic samples (air saturated). In both cases the relaxation kinetics are virtually independent of the monitoring wavelength. A value of $\tau = 9$ μs for the ^{3}Car decay in the anaerobic sample is in perfect agreement with data reported in the literature (Peterman et al., 1995; Siefermann-Harms and Angerhofer, 1995, 1998). Differences exist with respect to the values measured in aerobic samples. The data of Fig. 3 are described by a monoexpo-

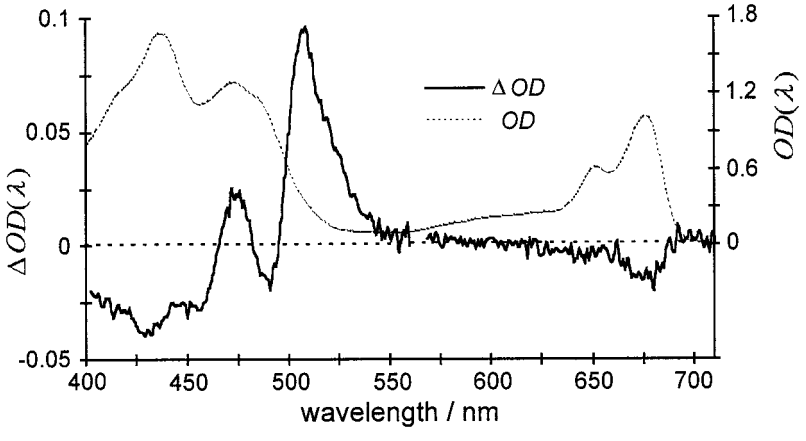

FIGURE 2 T − S spectra of solubilized LHCII at room temperature. The intensity of the pump pulse at 645 nm was ~10^{17} photons cm^{-2} $pulse^{-1}$. The delay between pump and probe pulse was 50 ns. The dotted curve represents the absorption spectrum of the sample. For further details see Materials and Methods.

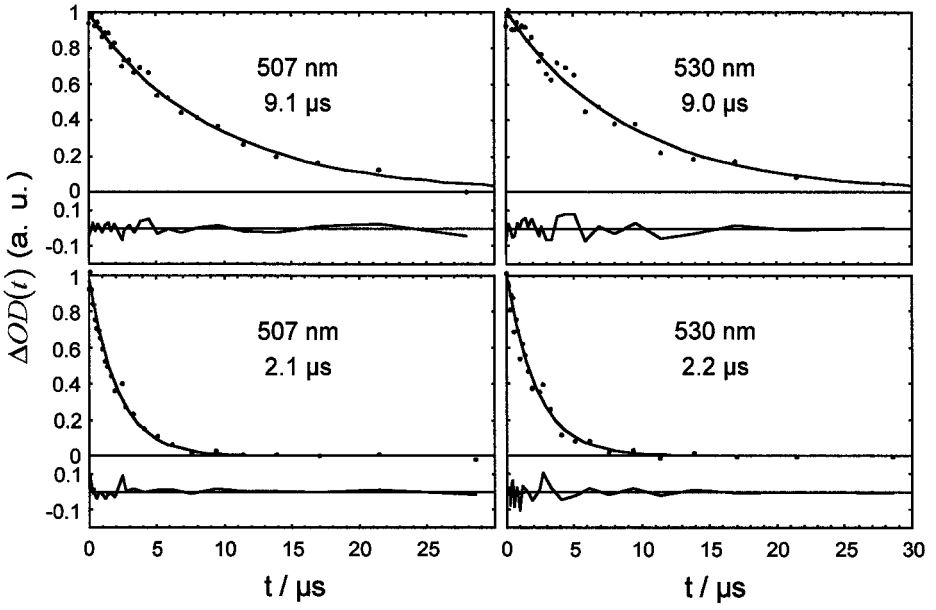

FIGURE 3 Flash-induced absorption changes at 507 nm (*left*) and 530 nm (*right*) as a function of the delay time between pump and probe pulses in solubilized LHCII under anaerobic conditions (*top*) and aerobic (air-saturated) conditions (*bottom*). The solid curves represent monoexponential fits with lifetimes given in the figure. For experimental details see Materials and Methods.

nential kinetics of ~2 μs at both wavelengths. A biphasic decay with $\tau = 2$ μs and 4 μs was reported by Peterman et al. (1995) with the former dominating at 505 nm and the latter at 528 nm. Somewhat slower values of ~7 μs were found by Siefermann-Harms and Angerhofer (1995, 1998). The kinetics become accelerated to 4 μs after sample treatment with linoleic acid. Based on these findings it was inferred that the protein matrix forms a barrier that restricts the accessibility of ^{3}Car to O_2 (Siefermann-Harms and Angerhofer, 1995, 1998).

Therefore, the most simple explanation for discrepancies between the data obtained for the decay kinetics under aerobic conditions is the existence of differences in the accessibility to O_2 due to sample heterogeneity. This idea is in line with the observation that the low-temperature fluorescence spectra of aggregated LHCII significantly depend on the mode of preparation of solubilized LCHII (Valsil'ev et al., 1997a,b). Therefore, additional experiments are required to analyze the specific effect of O_2 on the lifetime of carotenoid triplets.

Regardless of this O_2-dependent phenomenon, the above mentioned variations are without influence on the rise kinetics of the carotenoid triplet population. To check for a possible effect of the pump pulse intensity, experiments were performed at I_P values that cover a range of four orders of magnitude. The results obtained are depicted in Fig. 4. In this case the decay is somewhat slower (~4 μs) probably due to incomplete air saturation of the sample (it has to be mentioned that the experiments of Fig. 4 where performed with LHCII batches that were neither air saturated nor exposed to nitrogen gas). The traces depicted in Fig. 4 clearly show that the relaxation kinetics are independent of I_P up to very high values of 10^{18} photons cm^{-2} pulse^{-1}.

Kinetics of carotenoid triplet formation

The experiments were performed with pump and probe pulses of the same wavelength (one-color type) using an optical delay between pump and probe pulse as described in Materials and Methods.

Determination of the apparatus function

To analyze the time response of the apparatus, experiments were performed with a model system. In a solution of Chl *b* in 80% acetone the flash-induced change of the optical density was measured at 460 nm. At this wavelength a severe ground-state bleaching can be observed with only slight interference by chlorophyll triplet and excited state absorption. Fig. 5 shows the experimental data for the flash-induced ΔOD (460 nm) as a function of the delay time between pump and probe pulse. A characteristic time course of the ΔOD (460 nm) decrease monitored by the probe pulse is observed that is centered around zero delay time. The fit of the data was performed in the following way. Taking into account the fast internal conversion of higher excited into the first excited singlet states, the absorption coefficient α is given by

$$\alpha = \underbrace{\sigma_0(N - n_1 - n_T)}_{\text{ground state bleaching}} + \underbrace{\sigma_1 n_1}_{\text{excited singlet state absorption}} + \underbrace{\sigma_T n_T}_{\text{triplet state absorption}} \quad (3)$$

where n_i are the population densities of the first excited singlet ($i = 1$) and the triplet ($i = T$) state of Chl *b*, respectively (concentration in units of cm^{-3}), and σ_0, σ_1, and σ_T are the absorption cross sections of the ground, first excited singlet, and triplet state, respectively. The pump-

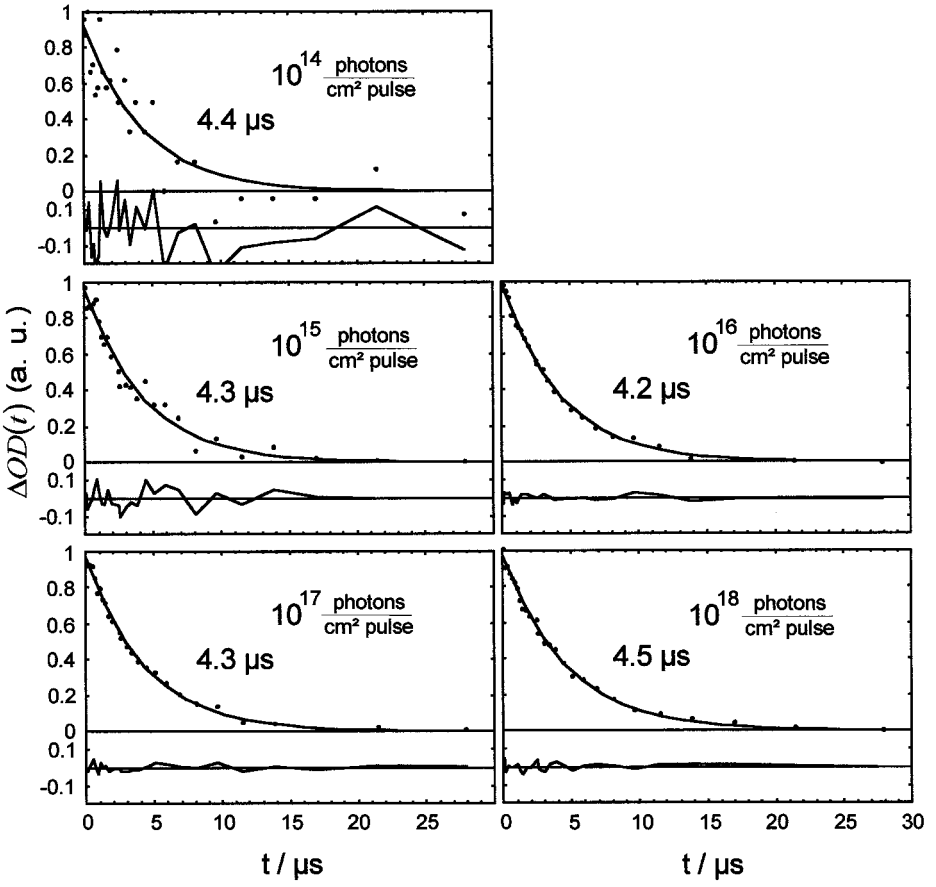

FIGURE 4 Flash-induced absorption changes at 507 nm as a function of the delay time between pump and probe pulses in solubilized LHCII under aerobic conditions. The intensity of the actinic pump pulse is given in the inset. The solid curves represent a monoexponential fit of the data with lifetimes that are given in the inset. In the lower part of each trace the fit quality is shown. For experimental details see Materials and Methods.

pulse-induced change of α is given by $\Delta\alpha = \alpha - \alpha_0$ where α_0 is the linear absorption coefficient. Thus, $\Delta\alpha$ can be calculated by the following equation:

$$\Delta\alpha = n_1(\sigma_1 - \sigma_0) + n_T(\sigma_T - \sigma_0) \quad (4)$$

The value of σ_T at 460 nm was calculated from the T − S spectrum of Chl *b* and the spectrum of the optical density (data not shown) to be approximately a factor of 5 lower than σ_0. Information about the excited state absorption cross section σ_1 at 460 nm was obtained from measurements at zero delay time, where the population of n_1 is considerably higher than n_T. Thus, $\Delta\alpha$ is dominated by the term $\Delta\alpha = n_1(\sigma_1 - \sigma_0)$, and therefore it is possible to calculated the ratio σ_1/σ_0 from $(N/n_1)(\Delta OD/OD_0) + 1$ where n_1 was calculated from Eq. 5, a and b (below). We found σ_1/σ_0 to be in the order of 0.1 (upper limit, 0.3). Based on this finding it is inferred that effects owing to excited singlet state absorption are of minor relevance. As a consequence of the rather small contribution of σ_1 and σ_T compared with σ_0 the decrease of ΔOD at 460 nm is understood to be predominantly caused by ground state depletion. The formation of excited singlets and triplets of Chl *b* can be described by the following equations:

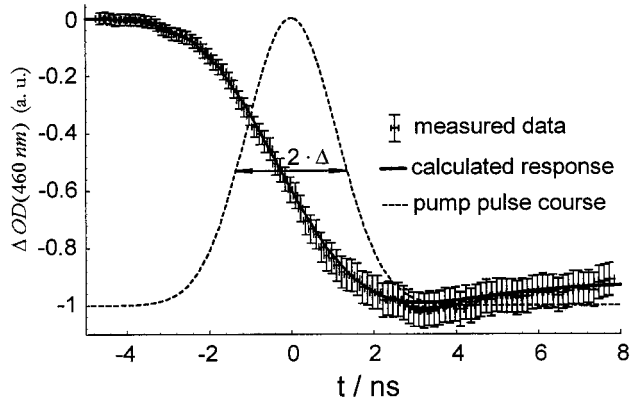

FIGURE 5 Flash-induced $\Delta OD(t)$ at 460 nm of Chl *b* in solution as a function of the optical delay time between pump and probe pulse. The model-based fit of $\Delta OD(t)$ is represented by a solid curve; the dashed curve describes the Gaussian profile of the pump pulse according to the fit.

$$\frac{d}{dt}n_1(t) = \sigma_0 i^{pump}(t)[N - n_1(t) - n_T(t)] - kn_1(t) \quad (5a)$$

$$\frac{d}{dt}n_T(t) = k_{ISC}n_1(t) - k_T n_T(t), \quad (5b)$$

where *k* is the reciprocal lifetime of Chl *b* singlets that was found to be 3 ns in acetonic solution (Pfarrherr et al., 1991). This value together with a triplet yield of 88% for Chl *b* in vitro (Bowers and Porter, 1967) leads to an intersystem crossing rate constant of $k_{ISC} = (3.4\ ns)^{-1}$. $i^{pump}(t)$ is the

time course of the pump pulse intensity assuming a Gaussian shape according to Eqs. 1 and 2. Actinic effects owing to the probe pulse can be neglected (see Experimental Setup).

For the calculation of ΔOD the profile of the nanosecond flashes has to be taken into account explicitly. Accordingly, the change of the optical density is given by (for details see Appendix):

$$\Delta OD(t) = -const \times \lg\left[\int_{-\infty}^{+\infty} \exp[-\Delta\alpha(t')d]\Gamma(t - t')dt'\right] \quad (6)$$

For the best fit of the data of ΔOD at 460 nm an arbitrary shift δ of the data with respect to the time axis was allowed. The result of this procedure is the solid curve that nicely fits the data with a value of $\delta = -0.2$ ns as shown by the solid curve in Fig. 5. To test the fit procedure, also the width Δ of the Gaussian shape (see Eqs. 1 and 2) was used as a free-running parameter. The best fit was obtained with $\Delta = 1.1$ ns. This value perfectly corresponds with the experimentally determined pulse width (see Materials and Methods).

The temporal evolution of singlet and triplet states together is responsible for the bleaching in Chl *b* in solution. This is illustrated by simulation curves shown in the Appendix (see Fig. 8). The most striking feature is the pronounced shift of the Chl *b* triplet population with respect to the bleaching at arbitrary amounts of k_{ISC}.

Measurements with solubilized LHCII

The measurements were performed as one-color experiments at 507 nm where the T − S difference spectrum of carotenoids exhibits a pronounced maximum (see Fig. 2). Based on the calibration measurement of the delay line (see Fig. 5) the data have to be shifted by the value of $\delta = -0.2$ ns. To avoid interference with nonlinear effects, the measurements were performed at a comparable low pump intensity of $\sim 10^{15}$ photons cm^{-2} $pulse^{-1}$ at 507 nm. Check experiments at higher pump intensities revealed that under these conditions the rise kinetics are not affected by nonlinear effects (data not shown). It was carefully checked by comparative fluorescence measurements (as described in Schödel et al., 1996) that saturation effects can be neglected (data not shown).

Fig. 6 shows the measured rise of $\Delta OD(t)$ at 507 nm in solubilized LHCII. For the sake of direct comparability the apparatus function for Chl *b* bleaching at 460 nm is also depicted in Fig. 6 as the inverted ΔOD curve of Fig. 5. An inspection of both curves readily shows that the rise of $\Delta OD(t)$ at 507 nm in solubilized LHCII is distinctly slower. To unravel the origin of this behavior, a detailed model-based data analysis is required. At first it has to be emphasized that the Chl *b* bleaching curve reflects the time-dependent population of singlets plus triplets and therefore exhibits a markedly faster kinetics than the calculated formation of Chl *b* triplets (via intersystem crossing) in solution (see Appendix). Second, it is most important to notice that the only significant route for population of the ^{3}Car state in solubilized LHCII is the triplet transfer from ^{3}Chl because the yield via direct intersystem crossing from singlets is in general vanishingly small for carotenoids (Frank and Cogdell, 1996; Koyama et al., 1996). Furthermore, in LHCII the very efficient singlet-singlet excitation energy transfer from carotenoids to chlorophylls (Connelly et al., 1997; Peterman et al., 1997a) and the short lifetime of carotenoid singlets (Frank and Cogdell, 1996; Koyama et al., 1996) prevent any significant population of carotenoid triplet states by any route that does not include the transient formation of chlorophyll triplets.

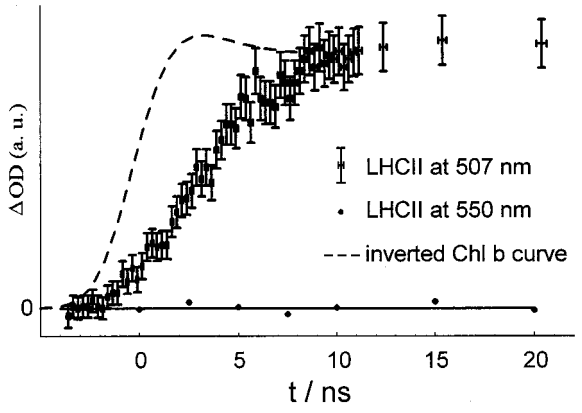

FIGURE 6 $\Delta OD(t)$ at 507 nm as a function of delay time between the pump (10^{15} photons cm^{-2} $pulse^{-1}$) and probe pulse in solubilized LHCII. The dashed line represents the inverted curve of the Chl *b* bleaching at 460 nm (see Fig. 5). The points are values measured at 550 nm at the same density of absorbed photons that are scaled by the same factor as $\Delta OD(t)$ at 507 nm. For further details see Material and Methods and text.

Based on the above mentioned considerations it is evident that the time course of ^{3}Car formation is basically described by the law of a sequential reaction of the type:

$$\begin{array}{ccccc} {}^1\text{Chl}^* & \xrightarrow{k_{ISC}} & {}^3\text{Chl} & \xrightarrow{k_{TT}} & {}^3\text{Car} \\ \downarrow k_\Sigma & & & & \\ {}^1\text{Chl} & & & & \end{array} \quad , \quad (7)$$

where $k = k_\Sigma + k_{ISC}$ and k_{TT} are the rate constants for the singlet state decay and triplet triplet transfer to carotenoids, respectively. Furthermore, the decay of ^{3}Car occurs via microsecond kinetics (see Figs. 3 and 4) and can be ignored for the analysis of ^{3}Car formation. Therefore, for the case of an instantaneous formation of ^{1}Chl* by a δ pulse and triplet transfer from ^{3}Chl to Car with an unlimited rate ($k_{TT} \to \infty$), the time dependence of ^{3}Car, $n_T^{Car}(t)$, would exhibit a mono-exponential rise with $\tau = k^{-1}$, where k is known to be 4.3 ± 0.2 ns for solubilized LHCII (Liu et al., 1993; Vasil'ev et al., 1997a,b). Any decrease of k_{TT} to finite values will give rise to a sigmoidal shape of the rise curve for $n_T^{Car}(t)$. These qualitative considerations show that the formation of ^{3}Car is limited by a rate constant of $(4.3 \pm 0.2 \text{ ns})^{-1}$ and that the

value of k_{TT} can be extracted from the time course of ΔOD at 507 nm.

For a quantitative evaluation it is necessary to perform a detailed analysis that takes into account the optical properties of the sample at 507 nm and the particular formation kinetics of ^{1}Chl* by excitation with nanosecond pulses.

The absorption coefficient α is given by

$$\alpha = \underbrace{\sigma_0^{Chl}(N^{Chl} - n_1^{Chl} - n_T^{Chl})}_{\text{Chl ground state bleaching}} + \underbrace{\sigma_1^{Chl} n_1^{Chl}}_{\text{excited Chl singlet state absorption}} + \underbrace{\sigma_T^{Chl} n_T}_{\text{Chl triplet state absorption}} + \underbrace{\sigma_0^{Car}(N^{Car} - n_T^{Car})}_{\text{Car ground state bleaching}} + \underbrace{\sigma_T^{Car} n_T^{Car}}_{\text{Car triplet absorption}}, \quad (8)$$

where n_i are the population densities of the singlet ($i = 1$) and the triplet ($i = T$) states of chlorophylls (Chl) and carotenoids (Car), respectively (concentration in units of cm^{-3}); σ_0, σ_1, and σ_T are the absorption cross sections of the ground, excited singlet, and triplet state, respectively. The linear absorption coefficient α_0 of LHCII is given by:

$$\alpha_0 = \sigma_0^{Chl} N^{Chl} + \sigma_0^{Car} N^{Car} \quad (9)$$

Thus, the flash-induced change of the absorption coefficient $\Delta\alpha = \alpha - \alpha_0$ can be calculated by the following equation:

$$\Delta\alpha = \underbrace{n_1^{Chl} \cdot (\sigma_1^{Chl} - \sigma_0^{Chl})}_{A} + \underbrace{n_T^{Chl} \cdot (\sigma_T^{Chl} - \sigma_0^{Chl})}_{B} + \underbrace{n_T^{Car} \cdot (\sigma_T^{Car} - \sigma_0^{Car})}_{C} \quad (10)$$

An inspection of Eq. 10 readily shows that the experimentally detected time course of the flash-induced change of the optical density ΔOD (507 nm) as a measurement of $\Delta\alpha(t)$ directly reflects the kinetics of carotenoid triplet formation provided that the contributions of terms A and B are negligibly small compared with the term C. To analyze possible contributions of terms A and B, comparative measurements were performed at 550 nm where term C is close to zero because at this wavelength the change of the absorption due to ^{3}Car population is negligibly small (see Fig. 2). On the other hand, the difference spectra for Chl triplet formation (den Blanken et al., 1983) and singlet state absorption are very flat in the range of 505–550 nm so that the values of terms A and B are approximately the same at 507 and 550 nm. Therefore, term C can be determined as the difference between the time courses of ΔOD (507 nm) and ΔOD (550 nm) measured at the same density of absorbed photons. The data obtained at 550 nm scaled with the same factor as ΔOD (507 nm) are shown in Fig. 6 as points. It readily shows that the contribution of terms A and B is rather small so that within the limits of the experimental error the flash-induced rise of ΔOD (507 nm) describes the kinetics of ^{3}Car formation. Accordingly, the rate constant for triplet transfer from ^{3}Chl to Car can be gathered from a numerical fit of the data to the differential equations that describe the time dependent populations n_i.

As discussed in the Appendix, the contribution of carotenoid ground state absorption (at 507 nm) for the generation of excited (chlorophyll) singlets n_1 does not effect the (normalized) evolution $n_1(t)$ as the singlet-singlet transfer from carotenoids to chlorophylls is ultra-fast (Peterman et al., 1997a). Accordingly, an effective optical cross section σ_0 can be used and the following equation is obtained (see Appendix):

$$\frac{d}{dt} n_1^{Chl} = i^{pump}(t)\sigma_0 - k n_1^{Chl}, \quad (11)$$

where k is the reciprocal lifetime of n_1 and $i^{pump}(t)$ is the pump pulse intensity profile that is given by Eq. 1.

An inspection of Eq. 11 readily shows that the time course of n_1^{Chl} is directly affected by two factors: 1) the value of k and 2) the intensity and shape of the actinic nanosecond flash. The rate constant strongly depends on the aggregation state of the sample. Therefore, it was carefully checked that effects owing to aggregation can be excluded (see Materials and Methods). All experiments performed with solubilized LHCII revealed that more than 90% of the chlorophyll singlets are characterized by a decay time of 4.3 ± 0.2 ns (Liu et al. 1993; Vasil'ev et al. 1997a,b). For an analysis of effects originating from $i^{pump}(t)$, two possible effects have to be considered, i.e., a faster rise of n_1^{Chl} with increasing I_P of nanosecond pulses and possible effects on the singlet state decay owing to annihilation. To obtain a sufficient signal-to-noise ratio a pump pulse intensity of 10^{15} photons cm^{-1} $pulse^{-1}$ had to be applied. Under this condition the fluorescence yield of the pump pulse was decreased by ~50% (see Schödel et al., 1996), indicating the onset of significant excited singlet state annihilation. As previously shown by Nordlund and Knox (1981) the fluorescence kinetics of LHCII remains virtually unaffected by high laser pulse intensities (see also Liu et al., 1993), thus indicating a practically instantaneous annihilation if more than one photon is absorbed during the excitation pulse (for discussion see Mauzerall, 1976; Gülen et al., 1986; Schödel et al., 1996). Accordingly, effects of I_P on the value of k can be excluded, and only the rise of $n_1^{Chl}(t)$ has to be analyzed. The results shown in the Appendix indicate that the data of Fig. 6 are very close to the low-intensity limit of I_P.

At the pump intensities of 10^{15} photons cm^{-1} $pulse^{-1}$ the extent of ΔOD at 507 nm is rather small (~3%) compared with that measured at high pump intensities (the decay kinetics remain invariant; see Fig. 4). Therefore, possible saturation effects concerning the population of carotenoid triplets can be excluded. The evolution of triplets $n_T^{Chl/Car}$ can be calculated using the following differential equations:

$$\frac{d}{dt} n_T^{Chl}(t) = k_{ISC} n_1^{Chl}(t) - k_T^{Chl} n_T^{Chl}(t) - k_{TT} n_T^{Chl}(t) \quad (12a)$$

$$\frac{d}{dt} n_T^{Car}(t) = k_{TT} n_T^{Chl}(t) - k_T^{Car} n_T^{Car}(t), \quad (12b)$$

where k_{ISC} is the rate constant for intersystem crossing from chlorophyll singlets into the triplet state and $k_T^{Chl/Car}$ that for the relaxation rates of corresponding triplets into the ground state. The influence of the latter rates is negligible in the nanosecond timescale as the relaxation via $k_T^{Chl/Car}$ occurs in the micro- and millisecond time range; k_{TT} is the rate constant for triplet-triplet transfer from ^{3}Chl to Car.

To model the experimental data by the solution of Eq. 12, a and b, ΔOD at 507 nm was calculated from $\Delta\alpha(t)$ using Eq. 6.

As shown in Fig. 7, the use of values for k_{TT} of $(10\ ns)^{-1}$ reported in the literature (Kramer and Mathis, 1980) leads to a totally unsatisfactory result (dotted curve). This problem cannot be resolved by variation of k_{ISC} within the range of permitted values because there is virtually no influence on the model curve (data not shown). As shown by the dashed and solid curves, a perfect description of the experimental data can be achieved when the rate constant k_{TT} is drastically enhanced. A qualitative inspection of the data reveals that k_{TT} has to be larger by at least one order of magnitude than the currently accepted value. Quantitative estimations lead to the conclusion that the lower limit of k_{TT} is $(0.5\ ns)^{-1}$.

As a consequence of this result, the interaction between Chl and Car in LHCII is stronger than currently assumed. An important implication of this finding is the conclusion that the protective action of carotenoids is much faster because the increase of k_{TT} by a factor of at least 20 causes a drastic decrease of the population probability of ^{3}Chl and thereby of the sensitized formation of harmful singlet oxygen.

CONCLUDING REMARKS

A detailed investigation of the flash-induced absorption changes at 507 nm in LHCII and model-based data analysis led to a lower limit of the rate constant for the transfer of triplets from Chl to Car. The result of $k_{TT} \geq (0.5\ ns)^{-1}$ reveals that the interaction between Chl and Car is stronger than currently assumed. This finding not only provides a simple explanation for the very fast singlet-singlet excitation energy transfer from Car to Chl but also illustrates the very high protective efficiency of carotenoids in LHCII.

APPENDIX

Calculation of a model curve for $\Delta OD(t)$ from $\Delta\alpha(t)$

We consider a sample with a time-dependent transmittance T that was induced by a pump pulse. A probe pulse passes this sample at the delay time t with respect to the pump pulse. The course of the probe pulse before passage is $i_0^{probe}(t' - t)$. The integral probe pulse intensity after passing the sample (at the time t) results from the temporal convolution of the probe pulse with the transmittance: $I_T^{probe}(t) = \int_{-\infty}^{+\infty} T(t') i_0^{probe}(t' - t)dt'$. Using Eq. 1, we obtain the fraction of the probe pulse intensity transmitted through the sample:

$$I_T^{probe}(t)/I_0^{probe} = \int_{-\infty}^{+\infty} T(t')\Gamma(t' - t)dt', \qquad (A1)$$

where the time-dependent transmittance is given by $T(t') = \exp[-\alpha(t')d]$, with α = absorption coefficient and d = the optical pathway of the sample. As $\alpha = \alpha_0 + \Delta\alpha(t)$, we obtain:

$$\frac{I_T^{probe}(t)/I_0^{probe}}{T_0} = \int_{-\infty}^{+\infty} \exp[-\Delta\alpha(t')d]\Gamma(t - t')dt', \qquad (A2)$$

where $T_0 = \exp[-\alpha_0 d]$ is the linear transmittance of the sample. Eq. A2 provides an expression that corresponds to the experimental data of the relative change of the sample transmittance $T^{rel}(t)$ (see Experimental Setup), Using the relation $\Delta OD = -\lg T^{rel}(t)$ Eq. A2 leads to Eq. 6.

Evolution of singlets and triplets in the case of Chl *b* in solution

Fig. 8 shows the transient populations of excited singlet and triplet states in Chl *b* solution calculated with the parameters used in Fig. 5. The

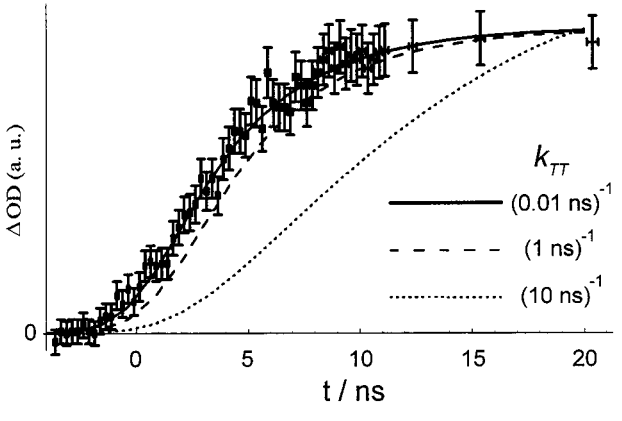

FIGURE 7 $\Delta OD(t)$ at 507 nm in solubilized LHCII as a function of delay time between the pump and probe pulse. The calculated curve with different k_{TT} values is represented by dotted ($k_{TT} = (10\ ns)^{-1}$), dashed ($k_{TT} = (1\ ns)^{-1}$), and solid ($k_{TT} = (0.01\ ns)^{-1}$) curves. The latter curve represents the case $k_{TT} \to \infty$.

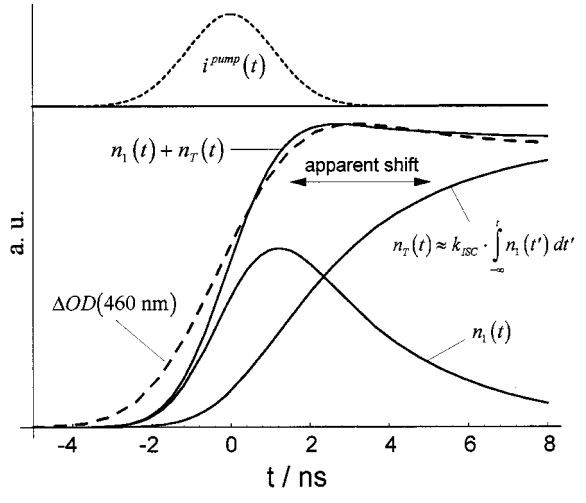

FIGURE 8 The evolution of singlet and triplet states in Chl *b* in solution.

inverted experimental bleaching curve (indicated by the dashed curve in Fig. 8) resembles the sum of $n_1(t)$ and $n_T(t)$ because the values of the absorption cross sections σ_1 and σ_T estimated at 460 nm are markedly smaller than σ_0 and therefore $\Delta\alpha \approx -\sigma_0(n_1 + n_T)$ (see Eq. 4). The main differences between both curves is because of the use of a nanosecond probe pulse that averages over a finite time interval (see Eq. 6).

To illustrate the time delay between bleaching and population of the Chl *b* triplet state, the time course of $n_T(t)$ is separately shown in Fig. 8. The triplet decay in Eq. 5b can be omitted because this process is orders of magnitude slower than the formation. Therefore, $n_T(t)$ (at the nanosecond timescale) also can be obtained from $n_T(t) = k_{ISC}\int_{-\infty}^{t} n_1(t')dt'$. For the sake of direct comparison, both curves, the experimental bleaching and $n_T(t)$, are normalized to the same maximal value.

Effective absorption cross section in LHCII at 507 nm

The rate equation for n_1^{Chl} at low pump intensities is given by:

$$\frac{d}{dt} n_1^{Chl} = i^{pump}(t)\sigma_0^{Chl}N^{Chl} - k^{Chl}n_1^{Chl} + k_{SS}n_1^{Car}, \quad \text{(A3)}$$

where k_{SS} is a fast singlet-singlet transfer rate (Peterman et al., 1997a). Accordingly, the equation for the population of Car singlets is:

$$\frac{d}{dt} n_1^{Car} = i^{pump}(t)\sigma_0^{Car}N^{Car} - k^{Car}n_1^{Car} - k_{SS}n_1^{Car} \quad \text{(A4)}$$

The singlet transfer efficiency via k_{SS} is nearly 100% (Peterman et al., 1997b). Therefore, the relaxation of Car singlets via k^{Car} can be neglected. Likewise, the population probability of this state and its time derivative $(d/dt)n_1^{Car}$ are practically zero. A simple algebraic rearrangement leads to

$$\frac{d}{dt} n_1^{Chl} = i^{pump}(t)\left[\underbrace{\sigma_0^{Chl}N^{Chl} + \sigma_0^{Car}N^{Car}}_{\text{linear absorption coefficient } \alpha_0}\right] - k^{Chl}n_1^{Chl}.$$

The term in the brackets is a sample constant that can be symbolized by σ_0, resulting in Eq. 11.

Effect of pump pulse intensity on the time course of Chl singlet states

Quantitatively, it is possible to describe the fluorescence saturation of small complexes by a model that involves the overall absorption cross section $\sigma_0^{complex}$ of the complex (Schödel et al., 1996). In the framework of this description, the absorption of more than one photon by the complex is looked upon as excited state absorption (of the complex). Consequently, the decrease of the fluorescence yield is due to a depletion of ground states of the complex. Thus, it is possible to investigate the influence of the pump intensity on the course of the evolution of excited states of the complex. Assuming that the relaxation of higher excited states happens fast, the kinetic equation for the complex is as follows:

$$\frac{d}{dt} n_1^{complex} = i_P(t)\sigma_0^{complex}(N^{complex} - n_1^{complex}) - n_1^{complex}k, \quad \text{(A5)}$$

where $n_1^{complex}/N^{complex}$ is the fraction of complexes that were already excited and k again is the reciprocal lifetime of singlet states of solubilized LHCII ($(4.3\ ns)^{-1}$). $\sigma_0^{complex} \approx 10^{-15}\ cm^2$ can be set for the absorption cross section of the complex at 507 nm (the absorbance at 507 nm is comparable with 645 nm, where $\sigma_0^{complex}$ was obtained from the fluorescence yield as a function of the excitation intensity; see Schödel et al., 1996).

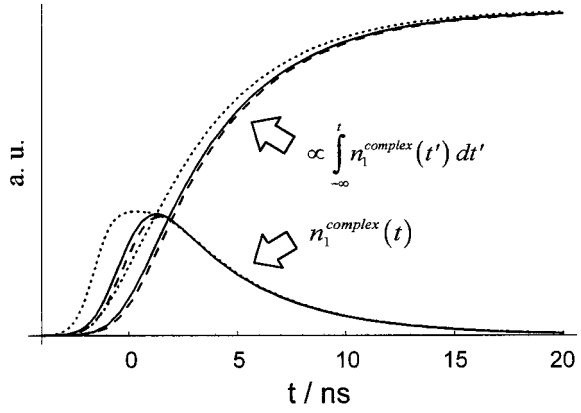

FIGURE 9 Calculation of excited chlorophyll singlets, $n_1(t)$, and integral amount as a function of time at different pulse intensities I_P in solubilized LHCII according to Eq. A12. The dashed line represents the low-intensity limit. The solid line corresponds to the intensity where ΔOD at 507 nm was measured (10^{15} photons cm^{-2} $pulse^{-1}$). The dotted curve shows the effect of high intensities (10^{16} photons cm^{-2} $pulse^{-1}$).

Fig. 9 shows the influence of the pump pulse intensity according to Eq. A5. Obviously, the deviation from the low-intensity limit is rather small at intensities of 10^{15} photons cm^{-2} $pulse^{-1}$. Only at 10^{16} photons cm^{-2} $pulse^{-1}$ is the evolution of singlets clearly affected.

As shown below, ΔOD at 507 nm is in accordance with the time integral over excited Chl singlets. It may be remarked that measurements of ΔOD at 507 nm performed at the pump intensity of 10^{16} photons cm^{-2} $pulse^{-1}$ are comparable with the dotted curve of Fig. 9.

Evolution of triplet states at solubilized LHCII

Fig. 10 shows the evolution of carotenoid triplet states (solid lines) as well as chlorophyll triplet states calculated at different rates of triplet-triplet transfer. Obviously, the curve of carotenoid triplets obtained in the limit

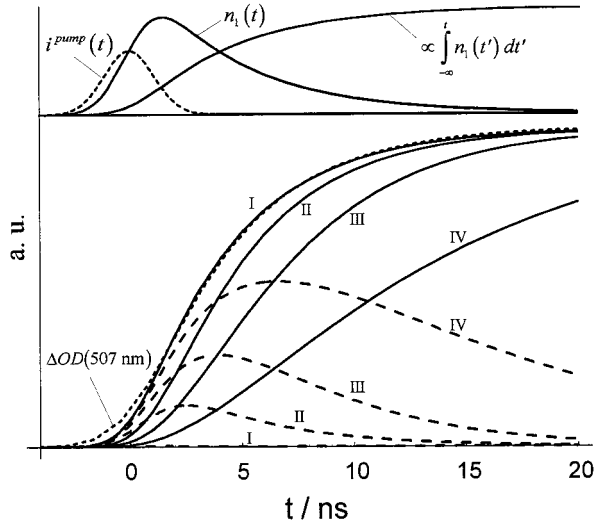

FIGURE 10 Calculation of the evolution of chlorophyll triplets (dashed lines) and carotenoid triplet states (solid lines) in solubilized LHCII at different rates k_{TT} (I: $(0.01\ ns)^{-1}$, II: $(1\ ns)^{-1}$, III: $(3\ ns)^{-1}$, IV: $(10\ ns)^{-1}$). The dotted curve corresponds to the experimental data of $\Delta OD(t)$ at 507 nm in solubilized LHCII. The upper curves indicate the time course of excitation and chlorophyll singlet population.

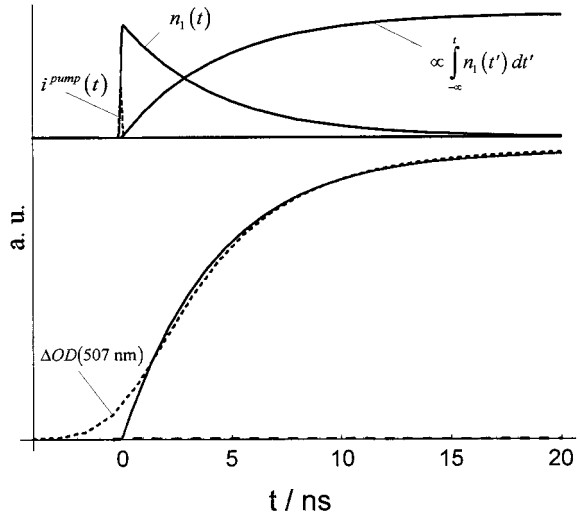

FIGURE 11 Calculation of the evolution of the carotenoid triplet state in solubilized LHCII assuming a 100-ps pulse as pump and probe source at a high rate $k_{TT} = (10\ \text{ps})^{-1}$. The upper curves indicate the time course of excitation and chlorophyll singlet population. The dotted curve corresponds to the experimental data of $\Delta OD(t)$ at 507 nm in solubilized LHCII.

$k_{TT} \rightarrow \infty$ (curve I, gathered at $k_{TT} = (0.01\ \text{ns})^{-1}$) is in good agreement with the data of ΔOD at 507 nm (the deviation with respect to the experimental data is due to the finite duration of the probe pulse (this effect was included for the calculation of the fits in Fig. 7 using Eq. 6). Curve I is in perfect agreement with the integral $\int_{-\infty}^{t} n_1(t')dt'$ plotted at the upper part of Fig. 10. This is illustrated in the following. In the case $k_{TT} \rightarrow \infty$ the chlorophyll triplets population, $n_T^{Chl}(t)$, remains very small (see Fig. 10) as once a chlorophyll triplet is generated it is transferred immediately to carotenoids. Therefore, also the derivative of $n_T^{Chl}(t)$ remains approximately zero. As the decay of $n_T^{Chl}(t)$ via k_T^{Chl} is negligible at the nanosecond timescale, we obtain $(d/dt)n_T^{Chl} = k_{ISC}n_1 - k_{TT}n_T^{Chl} \approx 0$. Thus, $n_T^{Chl}(t)$ is given by the relation $n_T^{Chl}(t) \approx (k_{ISC}/k_{TT})n_1(t)$. Also, the relaxation of carotenoid triplets is negligible at the nanosecond timescale. Therefore, the equation for carotenoid triplets is $(d/dt)n_T^{Car} = k_{TT}n_T^{Chl}$, resulting in:

$$n_T^{Car}(t) \cong k_{ISC} \int_{-\infty}^{t} n_1(t')dt' \qquad \text{(A6)}$$

Equation A6 reveals that the rise carotenoid triplets for $k_{TT} \rightarrow \infty$ is identical with the rise of Chl *b* triplets in Chl *b* in solution (see above).

Fig. 11 illustrates the case $k_{TT} \rightarrow \infty$ for a δ-like pump pulse. Obviously, the rise of carotenoid triplets occurs in a comparable way as in Fig. 10. Again, the integral $\int_{-\infty}^{t} n_1(t')dt'$ leads to a rise of the carotenoid triplet population that reflects the decay of chlorophyll singlets. Thus, experiments with shorter pulses (as those used in the current study) had to be performed at the same timescale of up to 20 ns. Therefore, the time resolution of these kinds of experiments is dependent mostly on the quality of the optical delay line.

We thank F. Hillmann and K. Palis for designing the device of the programmable electronic delay and H. Smolian for the HPLC analysis of the carotenoids. We thank Prof. R. Cogdell and Dr. Hann-Jörg Eckert for helpful discussion.

The financial support by Deutsche Forschungsgemeinschaft (Sfb 312) is gratefully acknowledged.

REFERENCES

Allen, J. F., and A. Nilsson. 1997. Redox signalling and the structural basis of regulation of photosynthesis by protein phosphorylation. *Physiol. Plant.* 100:863–868.

Bassi, R., B. Pineau, P. Dainese, and J. Marquardt. 1993. Carotenoid-binding proteins of photosystem II. *Eur. J. Biochem.* 212:297–303.

Berthold, D. A., G. T. Babcock, and C. F. Yocum. 1981. A highly resolved, oxygen-evolving photosystem II preparation from spinach thylakoid membranes. *FEBS Lett.* 134:231–234.

Bowers, P. G., and G. Porter. 1967. Quantum yields of triplet formation in solutions of chlorophyll. *Proc. R. Soc. A.* 296:435–441.

Connelly, P. P., M. G. Müller, R. Bassi, R. Croce, and A. R. Holzwarth. 1997. Femtosecond transient absorption study of caroteinoid to chlorophyll energy transfer in the light-harvesting complex II of photosystem II. *Biochemistry.* 36:281–287.

Demming-Adams, B., W. W. Adams III, B. A. Logan, A. S. Verhoevan. 1995. Xanthophyll cycle-dependent energy dissipation and flexible photosystem II efficiency in plants acclimated to light stress. *Aust. J. Plant. Physiol.* 22:249–260.

den Blanken, H. J., A. J. Hoff, A. P. J. M. Jongenelis, and B. A. Diner. 1983. High resolution triplet-minus-singlet absorbance difference spectrum of photosystem II particles. *FEBS Lett.* 157:21–27.

Foote, C. S. 1976. Photosensitized oxidation and singlet oxygen: consequences in biological systems. *In* Free Radicals in Biology, Vol. 2. W. A. Pryor, editor, Vol. II, Academic Press, New York. 85–133.

Frank, H. A., and R. Cogdell. 1996. Carotenoids in photosynthesis. *Photochem. Photobiol.* 63:257–264.

Gantt, E. 1986. Phycobilisomes. *In* Encyclopedia of Plant Physiology, New Series, Vol. 19. L. A. Staehelin and C. J. Arntzen, editors. Springer, Berlin. 260–268.

Green, B. R., and D. G. N. Durnford. 1996. Chlorophyll-carotenoid proteins of oxygenic photosynthesis. *Annu. Rev. Plant Physiol. Plant Mol. Biol.* 47:685–714.

Gülen, D., B. P. Wittmershaus, and R. S. Knox. 1986. Theory of picosecond-laser-induced fluorescence from highly excited complexes with small numbers of chromophores. *Biophys. J.* 49:469–477.

Heinze, I., E. Pfündel, M. Hühn, and H. Dau. 1997. Assembly of light harvesting complexes II (LHCII) in the absence of lutein: a study on the α-carotenoid-free mutant C-2A′-34 of the green alga *Scenedesmus obliquus. Biochim. Biophys. Acta.* 1320:188–194.

Hemelrijk, P. W., S. L. Kwa, R. van Grondelle, and J. P. Dekker. 1992. Spectroscopic properties of LHC-II, the main light-harvesting chlorophyll a/b protein complex from chloroplast membranes. *Biochim. Biophys. Acta.* 1098:159–166.

Horton, P., A. V. Ruban, and R. G. Walters. 1996. Regulation of light harvesting in green plants. *Annu. Rev. Plant Physiol. Plant Mol. Biol.* 47:655–684.

Irrgang, K.-D., E. J. Boekema, J. Vater, and G. Renger. 1988. Structural determination of the photosystem II core complex from spinach. *Eur. J. Biochem.* 178:209–217.

Jansson, S. 1994. The light harvesting chl a/b binding proteins. *Biochim. Biophys. Acta.* 1184:1–19.

Koyama, Y., M. Kuki, P. O. Andersson, and T. Gillbro. 1996. Singlet excited states and the light harvesting function of carotenoids in bacterial photosynthesis. *Photochem. Photobiol.* 63:243–256.

Kramer, H., and P. Mathis. 1980. Quantum yield and rate of formation of the carotenoid triplet state in photosynthetic structures. *Biochim. Biophys. Acta.* 593:319–329.

Kühlbrandt, W. 1994. Structure and function of the plant light-harvesting complex LHCII. *Curr. Opin. Struct. Biol.* 4:519–528.

Kühlbrandt, W., D. N. Wang, and Y. Fujiyoshi. 1994. Atomic model of plant light-harvesting complex by electron crystallography. *Nature.* 367: 614–621.

Liu, B., A. Napiwotzki, H.-J. Eckert, H. J. Eichler, and G. Renger. 1993. Studies on the recombination kinetics of the radical pair $P680^+Pheo^-$ in isolated PS II core complexes from spinach. *Biochim. Biophys. Acta.* 1142:129–138.

Mauzerall, D. 1976. Multiple excitations in photosynthetic systems. *Biophys. J.* 16:87–91.

Nordlund, T. M., and W. H. Knox. 1981. Lifetime of fluorescence from light harvesting chlorophyll a/b proteins excitation intensity dependence. *Biophys. J.* 38:193–201.

Nechustai, R., J. P. Thornber, L. K. Patterson, R. W. Fessenden, and H. Levanon. 1988. Photosensitization of triplet carotenoid in photosynthetic light-harvesting complex of photosystem II. *J. Phys. Chem.* 92: 1165–1168.

Paulsen, H. 1995. Chlorophyll a/b-binding proteins. *Photochem. Photobiol.* 62:367–382.

Peterman, E. J. G., F. M. Dukker, R. Van Grondelle, and H. Van Amerongen. 1995. Chlorophyll a and carotenoid states in light harvesting complex II of higher plants. *Biophys. J.* 69:2670–2678.

Peterman, E. J. G., C. C. Gradinaru, F. Calkoen, J. C. Borst, and R. van Grondelle. 1997b. Xanthophylls in light harvesting complex II of higher plants: light harvesting and triplet quenching. *Biochemistry.* 36: 12208–12215.

Peterman, E. J. G., S. Hobe, S. F. Calkoen, R. van Grondelle, H. Paulsen, and H. van Amerongen. 1996. Low temperature spectroscopy of monomeric and trimeric forms of reconstituted light-harvesting chlorophyll a/b complex. *Biochim. Biophys. Acta.* 1273:171–174.

Peterman, E. J. G., R. Monshouwer, I. H. M. van Stokkum, R. van Grondelle, and H. van Amerongen. 1997a. Ultrafast singlet excitation transfer from carotenoids to chlorophylls via different pathways in light-harvesting complex II of higher plants. *Chem. Phys. Lett.* 264:279–284.

Pfarrherr, A., K. Teuchner, and D. Leupold. 1991. Chlorophyll b in solution: fluorescence lifetimes, absorption and emission spectra as criteria of purity. *J. Photochem. Photobiol. B. Biol.* 9:35–41.

Porra, R. J., W. A. Thompson, and P. E. Kriedemann. 1989. Determination of accurate extinction coefficients and simultaneous equations for assaying chl a and b extracted with four different solvents: verification of the concentration of chl standards by atomic absorption spectroscopy. *Biochim. Biophys. Acta.* 975:384–394.

Renger, G. 1992. Energy transfer and trapping in photosystem II. *In* Topics in Photosynthesis, The Photosystems: Structure, Function and Molecular Biology. J. Barber, editor. Elsevier, Amsterdam. 45–99.

Schödel, R., F. Hillmann, T. Schrötter, K.-D. Irrgang, J. Voigt, and G. Renger. 1996. Kinetics of excited states of pigment clusters in solubilized light-harvesting complex II: photon density-dependent fluorescence yield and transmittance. *Biophys. J.* 71:3370–3380.

Siefermann-Harms, D. 1987. The light harvesting protective functions of carotenoids in photosynthetic membranes. *Physiol. Plant.* 69:561–568.

Siefermann-Harms, D., and A. Angerhofer. 1995. An O_2-barrier in the light-harvesting complex LHCII protects chlorophylls and carotenoids from photooxydation. *In* Photosynthesis: From Light to Biosphere, Vol. 4. P. Mathis, editor. Kluwer Akademic Publishers, Dordrecht, The Netherlands. 71–74.

Siefermann-Harms, D., and A. Angerhofer. 1998. Evidence for an O_2-barrier in the light-harvesting chlorophyll-a/b-protein complex LHCII. *Phot. Res.* 55:83–94.

Thornber, J. P., D. T. Morishige, S. Anandan, and G. F. Peter. 1991. Chlorophyll carotenoid proteins of higher plant thylakoids. *In* Chlorophylls. H. Scheer, editor. CRC Press, Boca Raton, FL. 549–585.

van Grondelle, R., J. P. Dekker, T. Gillbro, and V. Sundstrom. 1994. Energy transfer and trapping in photosynthesis. *Biochim. Biophys. Acta.* 1187:1–65.

Vasil'ev, S., K.-D. Irrgang, T. Schrötter, A. Bergmann, H.-J. Eichler, and G. Renger. 1997a. Quenching of chlorophyll a fluorescence in the aggregates of LHCII: steady state fluorescence and picosecond relaxation kinetics. *Biochemistry.* 36:7503–7512.

Vasil'ev, S., T. Schrötter, A. Bergmann, K.-D. Irrgang, H.-J. Eichler, and G. Renger. 1997b. Cryoprotectant-induced quenching of chlorophyll a fluorescence from LHCII in vitro: time-resolved fluorescence and steady state spectroscopic studies. *Photosynthetica.* 33:553–561.

Völker, M., T. A. Ono, Y. Inoue, and G. Renger. 1985. Effect of trypsin on PS II particles: correlation between Hill-activity, Mn-abundance and peptide pattern. *Biochim. Biophys. Acta.* 806:25–34.

Wellburn, A. R., and H. Lichtenthaler. 1984. Formulae and program to determine total carotenoids and chlorophylls a and b of leaf extracts in different solvents. *In* Advances in Photosynthesis Research, Vol. 2. C. Sybesma, editor. Martinus Nijhoff, The Hague, The Netherlands. 9–12.

Zucchelli, G., P. Dainese, R. C. Jennings, J. Breton, F. M. Garlaschi, and R. Bassi. 1994. Gaussian decomposition of absorption and linear dichroism spectra of outer antenna complexes of photosystem II. *Biochemistry.* 33:8982–8990.